NANO LETTERS

2007
Vol. 7, No. 10
2970−2975

Color-Changeable Optical Transport through Se-Doped CdS 1D Nanostructures

Anlian Pan,*,‡,§,† Xiao Wang,†,|| Pengbin He,‡ Qinglin Zhang,‡ Qiang Wan,‡ Margit Zacharias,§ Xing Zhu,||,⊥ and Bingsuo Zou‡

Micro-Nano Technologies Research Center, Hunan University, Changsha 410082, China, MPI of Microstructure Physics, Weinberg 2, Halle 06120, Germany, State Key Lab for Mesoscopic Physics, School of Physics, Peking University, Beijing 100871, China, and National Center for Nanoscience and Technology, Beijing, 100080, China

Received May 2, 2007; Revised Manuscript Received July 27, 2007

ABSTRACT

The optical-transport properties of 1D Se-doped CdS nanostructures with different doping contents and/or crystallization degrees are reported. The locally excited photoluminescence shows a significant redshift during the transport along the long axis of the 1D structures and can leave enough PL intensity for detection. The magnitude of the redshift is found to be highly dependent on the content of doping and the crystallization degree. The experimental results are compared with theoretical calculations based on the fundamental absorption rule of the semiconductor, which demonstrates that the redshift is related to the optical reabsorption effects induced by the local structural disorder in the semiconductors. Such optical properties of 1D semiconductor structures might be of interest for potential applications in color-tunable nanosized light-emitting and/or frequency-converting devices.

One-dimensional (1D) nanostructured materials are especially attractive as building blocks or for the assembly of integrated nanosystems because this kind of nanostructure can function as both device elements and interconnects.[1−5] Because of the strong optical confinement in the radial directions, semiconductor nanowires and nanobelts are found to have promising optical-transport properties. Their photoluminescence (PL) excited by light illumination can be effectively guided along their axis and leak out at their ends, which act as reflectors because of the difference in the reflective index between the medium and the surrounding circumstance.[6−8] This peculiarity makes this kind of nanostructure important for potential applications in nanophotonic devices or units, such as nanooptical fibers, optical waveguide cavities, and nanolasers.[6−13]

In polar semiconductors, the structural disorder from defects, impurities or phonons can induce an extension of the density of state into the band gap near the main edges of the bands, and optical transitions assisted by this extension of state give rise to an exponential tail near the fundamental absorption edge at the long wavelength direction (Urbach tail).[14,15] It was observed in bulk semiconductors or films that the Urbach tail can induce self-absorption of band-edge emission and then leads to a redshift of the PL spectrum.[16,17] However, such a self-absorption-induced PL redshift is not remarkable and is not easy to be observed in the normal bulk materials because the inherent PL cannot transport along single directions, and then the detected light is mainly from the in situ excitation position. 1D nanostructured semiconductors, like nanobelts or nanowires, provide a very good system for observing and studying the self-absorption-induced optical effect because the optical transport in these structures takes place preferentially along the long axis direction, and the positions for excitation and emission can be separated effectively, making the self-absorption effect much easier to observe and study.

In this work, we study the PL transport properties of 1D Se-doped CdS nanostructures with different doping contents or crystallizations and demonstrate that all of these nanostructures can produce a significant PL redshift in their respective spectral regions, with the redshift magnitude highly related to the content of doping and the crystallization of the structures. Calculation using the fundamental absorption rule of semiconductors and the Urbach rule shows that the redshift magnitude is greatly dependent on the degree

* Corresponding author. E-mail: pananlian@hotmail.com.
† These authors made equal contribution in this study.
‡ Hunan University.
§ MPI of Microstructure Physics.
|| Peking University.
⊥ National Center for Nanoscience and Technology.

10.1021/nl0710295 CCC: $37.00
Published on Web 08/29/2007

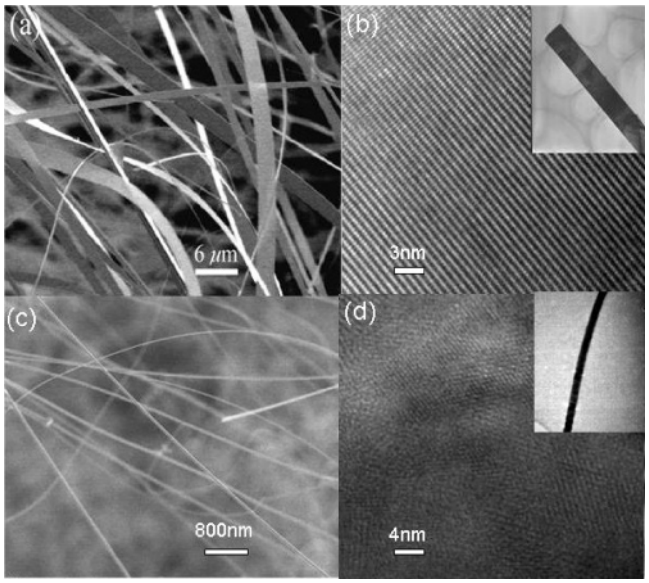

Figure 1. (a) Typical SEM image of the as-prepared nanobelts, (b) the HRTEM lattice image of a representative belt as well as its corresponding TEM morphology image (inset), (c) the SEM image of the as-prepared Se-doped CdS nanowires grown at low deposition temperatures, and (d) the HRTEM image and the corresponding TEM morphology image (inset) of a representative wire.

of local inhomogeneity-induced structural disorder in the materials, which is in good agreement with the observations in the experiments. This finding of broad color-changeable optical-transport behavior of 1D Se-doped CdS nanostructures may have great significance in constructing multifunctional nanodevices.

The Se-doped CdS nanostructures (nanobelts and nanowires) used in this study were synthesized by the metal-catalyzed physical evaporation route, which is described in detail elsewhere.[18] Figure 1a gives the typical SEM image of the as-prepared nanobelts, which indicates that the belts are very uniform along their long axis direction, with the width in the range of 1−5 μm and the depth being about 100 nm. The length of the belts can reach several hundred micrometers and even some of them can extend to the order of millimeters. Figure 1b shows the HRTEM lattice image of a representative belt as well as its corresponding TEM morphology image (inset), which demonstrates the single-crystal quality of the belts. Figure 1c shows the SEM image of the as-prepared Se-doped CdS nanowires grown at low deposition temperatures. The diameter of the wires is about 100−200 nm, and their length exceeds 1 mm. Figure 1d is the HRTEM image and the corresponding TEM morphology image (inset) of a representative wire. Different from the high-quality belts, the wires are very poorly crystallized (somehow like polycrystals), with obvious defects and lattice disorder. The compositions or doping content of the as-prepared nanostructures are obtained by comparing their XRD peak positions with those of the binary CdS and CdSe crystals and calculating the composition with the Vegard's relation (see Figure S1 in the Supporting Information).[18] The band gaps of the samples were estimated by their UV−vis absorption spectra (see Figure S2 in the Supporting Information).

The optical-transport properties of the 1D nanostructures were investigated using scanning near-field optical microscopy (SNOM). The experimental setup is shown schematically in Figure S3 (see the Supporting Information). Single nanobelts/wires were illuminated with a tightly focused laser beam (continuous-wave, 442 nm) at different local positions along various lengths relative to a NSOM collection tip (fiber probe) held stationary over one of their ends. Then the propagation-distance-dependent PL spectra can be studied effectively simply by moving the excitation laser beam.

Figure 2a−c shows, respectively, the far-field optical images of single excited $CdS_{0.65}Se_{0.35}$, $CdS_{0.82}Se_{0.18}$, and CdS nanobelts, collected with a color CCD camera in dark field. The left images are their in situ PL under laser illumination. Some of the PL is guided through the nanobelts and emitted at one of their ends (see the right optical images). The numbers give the distances between the excitation spots and the examined ends of the corresponding structures, respectively. It shows that the PL color of the heavily doped $CdS_{0.65}Se_{0.35}$ belts is changed from (original) orange to red after ~188 μm transport, and the PL color from the lightly doped $CdS_{0.82}Se_{0.18}$ belts is changed from (original) green to orange after ~225 μm transport, while the PL color from the undoped CdS belts has no apparent change after ~300 μm transport. Figure 2d shows the far-field PL images of an excited $CdS_{0.86}Se_{0.14}$ nanowire under laser illumination. The left image is the in situ PL, and the right two images are the PL collected at one of its ends with an excitation-detection distance of 20 and 150 μm, respectively. The PL color change of these poorly crystallized wires is more apparently observed, that is, from the original green changed to orange-yellow and red after ~20 μm and ~150 μm transport, respectively. Figure 2e gives the three-dimensional near-field optical image of the end emission from the doped wire, with the position of the excitation laser spot about 300 μm away from this emitting end. The down-right inset is the corresponding morphology image of the end. The results demonstrate that all of the examined nanostructures are very good waveguide cavities and the emitted light can be effectively transported several hundred micrometers along their long axes and still leave with considerable optical intensity.

Figure 3a shows the locally detected near-field PL spectra from a $CdS_{0.65}Se_{0.35}$ belt, with the excitation laser beam at different points of the nanobelt. This series of PL spectra record the distance-dependent photon transport properties of the belt. Apparently, the emission bands exhibit a significant redshift with increasing PL propagation distance along the belt. The other nanostructures with different doping contents all have a similar spectral redshift phenomena. Such spectral behavior is consistent with the observed far-field PL spot image (Figure 2a and b). Figure 3b shows the plots of redshift value in photon energy versus excitation position (transport distance) for $CdS_{0.65}Se_{0.35}$, $CdS_{0.82}Se_{0.18}$, and CdS nanobelts, respectively. From this figure, we can derive additional detailed information. First, the redshift with transport distance will finally saturate at a long enough distance. Second, the redshift value at the same transport distance is definitely

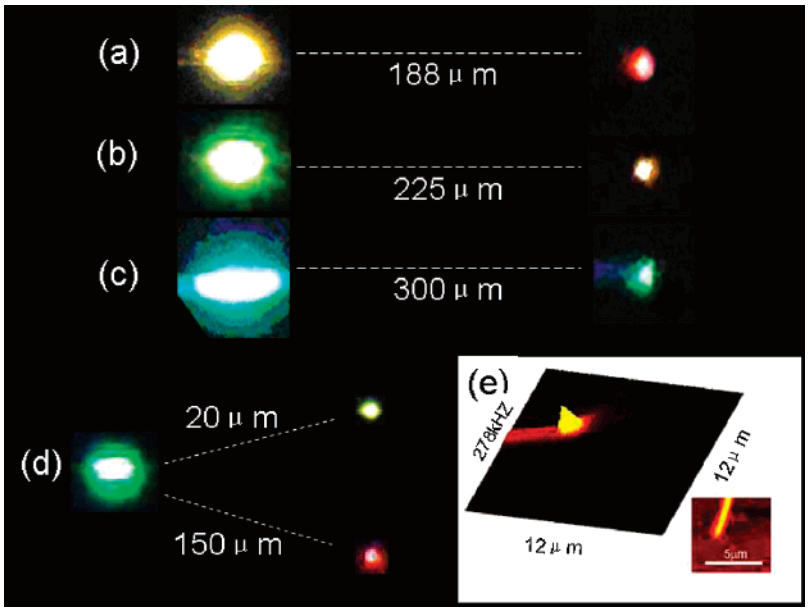

Figure 2. (a−c) Far-field optical images of single excited $CdS_{0.65}Se_{0.35}$, $CdS_{0.82}Se_{0.18}$, and CdS nanobelts, respectively: Left, the in situ PL images under laser illumination; right, the emission images of the examined ends. (d) The far-field PL image of an excited $CdS_{0.86}Se_{0.14}$ nanowire under laser illumination: Left, the in situ PL image; right, the end PL images with an excitation-detection distance of 20 and 150 μm, respectively. (e) The three-dimensional near-field optical image of the end emission from the doped wire, with an excitation-detection distance of about 300 μm; inset, the corresponding morphology image of the end.

different for belts with different doping contents. The larger the doping content, the larger the redshift magnitude produced. Third, the redshift maximum is also different. A heavily doped $CdS_{0.65}Se_{0.35}$ has a maximum redshift of ~60 meV, whereas the value for a lightly doped $CdS_{0.82}Se_{0.18}$ is ~42 meV and is only about 30 meV for an undoped CdS nanobelt. The inset of Figure 3b gives the plot of redshift versus excitation position for the $CdS_{0.86}Se_{0.14}$ wires, which shows a redshift maximum of ~170 meV. Apparently, the redshift of the poorly crystallized wires is more significant than those of the highly crystallized nanobelts, which is in good agreement with the observations in the far-field images.

Here we use the optical absorption theory of semiconductors to understand the observed optical-transport phenomenon, especially the composition- (doping) and defect-induced optical redshift in the 1D nanostructured system. The absorption coefficient α ($h\nu$) of a semiconductor can be defined by the following equation:[14,15]

$$\text{For } E \geq E_g,\ \alpha(h\nu)_I = A_0(E - E_g)^{1/2} \tag{1}$$

$$\text{For } E < E_g,\ \alpha(h\nu)_{II} = K_0 \exp\left[\frac{\sigma}{kT}(E - E_g)\right] \text{ (Urbach rule)} \tag{2}$$

In order to express the absorption coefficient α ($h\nu$) as a continuous function, eq 2 can be rewritten as[19]

$$\text{For } E < E_g,\ \alpha(h\nu) = A_0\sqrt{\frac{kT}{2\sigma}} \exp\left[\frac{\sigma}{kT}(E - E_{ch})\right] \tag{3}$$

where A_0 [$=2 \times 10^4$ $cm^{-1}(eV)^{-1/2}$] is a constant, E_g is the band gap energy, kT (=0.025 eV) is the thermal energy at room temperature, h is Planck's constant, υ is the photon frequency ($E = h\upsilon$), σ is a dimensionless phenomenological fitting parameter, and $E_{ch} = E_g + kT/2\sigma$ is the crossover energy. In solid materials, σ behaves as[20]

$$\sigma = \sigma_0 \frac{2kT}{h\omega_0} \tanh\left[\frac{h\omega_0}{2kT}\right] \tag{4}$$

with σ_0 and ω_0 as constants. On the other side, the absorption coefficient α ($h\upsilon$) in semiconductor can be defined by the following equation[21]

$$I(x) = I_0 e^{-\alpha(h\nu)x} \tag{5}$$

where I_0 and $I(x)$ are the optical intensities at the zero and x position, respectively. Therefore, by inserting eqs 1 and 3 into eq 4, we get the spectrum at the position x

$$S(x) = S_0 e^{-\alpha(h\nu)x} \tag{6}$$

where S_0 is the initial spectrum (zero position). Combining the above eqs 1, 3, and 6, the characteristics of PL spectrum at position x in a given semiconductor is finally determined by parameters ω_0 and σ_0. For the Se-doped CdS system at room temperature, $h\upsilon_0$ is around 36 meV[22] and can be seen as an invariable in this calculation, but σ_0 is variable with the inherent structure, and it is an indicator of the degree of disorder of crystalline materials.[22] The higher the degree of local disorder, the smaller the σ_0 value.

Figure 4a shows the initial PL spectrum of $CdS_{0.65}Se_{0.35}$ nanobelts under excitation (0 μm) as well as the theoretical

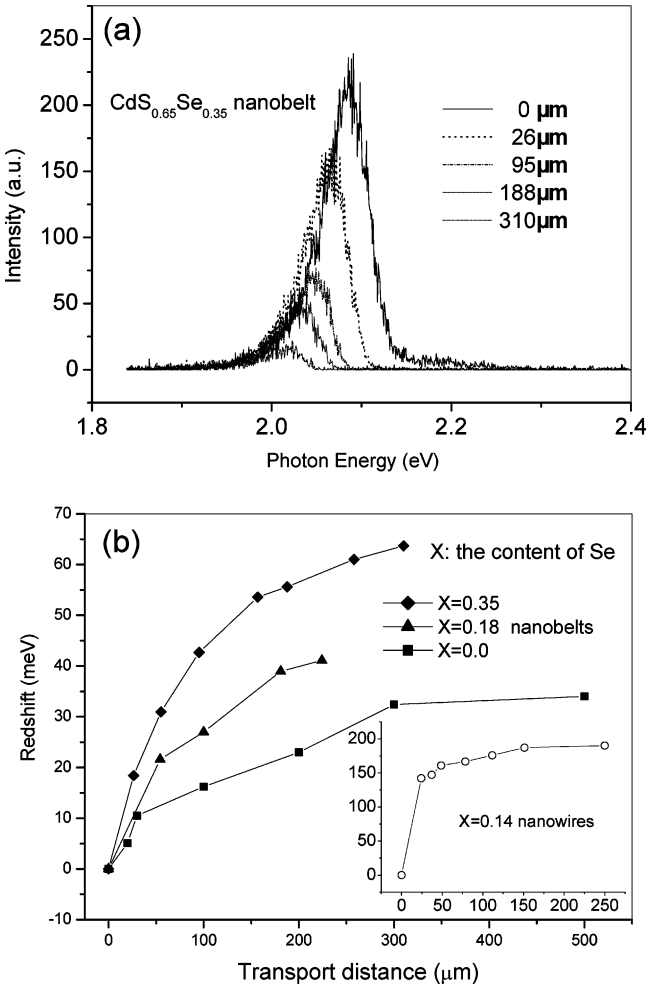

Figure 3. (a) Locally detected near-field PL spectra from a $CdS_{0.65}Se_{0.35}$ belt, with the excitation laser beam at different points of the nanobelt; (b) the plots of redshift value in photon energy vs excitation position (transport distance) for $CdS_{0.65}Se_{0.35}$ (curve 1), $CdS_{0.82}Se_{0.18}$ (curve 2), and CdS (curve 3) nanobelts, respectively; inset, the plot of redshift vs excitation position for the $CdS_{0.86}Se_{0.14}$ wires.

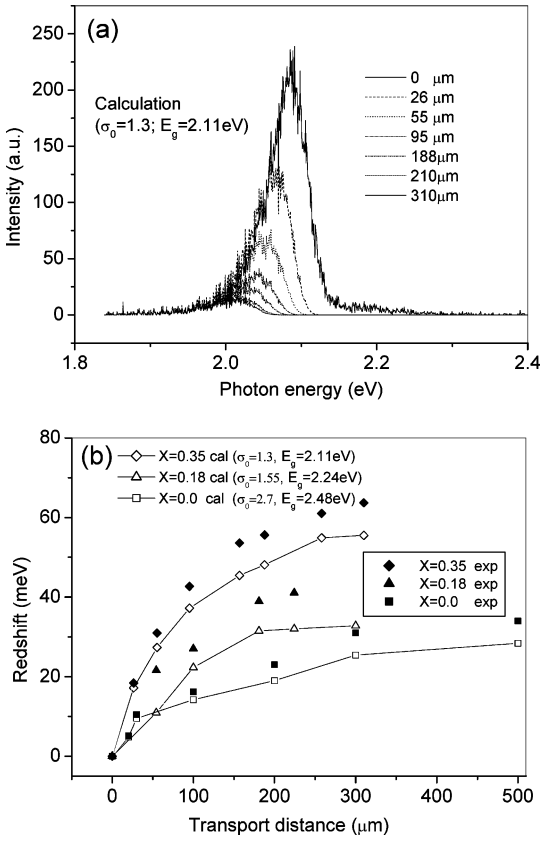

Figure 4. (a) Initial PL spectrum of $CdS_{0.65}Se_{0.35}$ nanobelts under excitation (0 μm) as well as the theoretical spectra at different transport distance; (b) the theoretical plots of redshift value in photon energy vs transport distance for $CdS_{0.65}Se_{0.35}$, $CdS_{0.82}Se_{0.18}$, and CdS nanobelts, respectively (broken lines), and the respective experimental value of $CdS_{0.65}Se_{0.35}$ (solid rhombus), $CdS_{0.82}Se_{0.18}$ (triangle), and CdS nanobelts (rectangle) for comparison.

spectra at different transport distances calculated using the above equations. Similar to the experimental results, the calculated spectra exhibit a significant redshift with increasing the transport distance (i.e., the x value in eq 5). The broken lines in Figure 4b show theoretical plots of the redshift value in photon energy versus transport distance for $CdS_{0.65}Se_{0.35}$, $CdS_{0.82}Se_{0.18}$, and CdS nanobelts, respectively. The respective value of parameter σ_0 used here is taken from the corresponding bulk single crystals with the same doping content.[22,23] The solid rhombus, triangle, and rectangle are the respective experimental values of $CdS_{0.65}Se_{0.35}$, $CdS_{0.82}Se_{0.18}$, and CdS nanobelts for comparison. Apparently, the theoretical results show some similar characteristics with those of our experiments; that is, the redshift will saturate after a long enough transport distance, and the heavily doped samples have a larger redshift magnitude than those of lightly or undoped ones. These consistencies between experiments and theory indicate that the PL redshifts are surely from the Urbach-tail-induced PL self-absorption effect in the belts. The difference in maximum redshift between the nanostructures with different doping contents should come from their differences of composition-related local structural disorder, which can be directly observed from comparing their UV−vis absorption spectra (Figure S4, see the Supporting Information). With increasing the Se doping content, the CdS-based nanostructures will have a broader absorption edge, which indicates an increase of the structural disorder degree induced by the composition fluctuation and an accompanying decrease of the σ_0 value. A larger disorder degree (i.e., smaller σ_0 value) can lead to a larger Urbach tail,[22] which will finally induce the PL spectrum to have a more-noticeable redshift during the light transport along the nanostructures. In addition, it is noted that the experimental observed redshift values are apparently somehow larger than those of theoretical results for all of the samples. Because the theoretical calculation is based on the σ_0 value of bulk single crystal, the disaccord could come from the structural difference between the 1D nanostructures and the corresponding bulk crystals. Because of the very small size in radial direction, the nanostructures may contain more defects at the surface region than the bulk. Because of this additional defect-related surface structural disorder, the nanobelts have a smaller σ_0 value than that of the bulk, leading to an observed redshift larger than the theoretical result (calculated with the bulk σ_0 value).

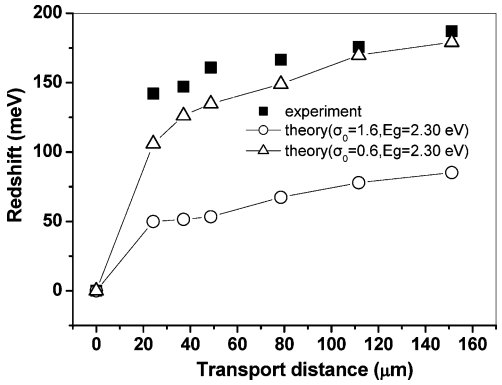

Figure 5. Theoretical results of redshift vs transport distance for the $CdS_{0.86}Se_{0.14}$ wires, calculated with $\sigma_0 = 1.6$ (for the corresponding bulk single crystal) and 0.6, respectively (broken lines), and the corresponding experimental value (solid rectangles) for comparison.

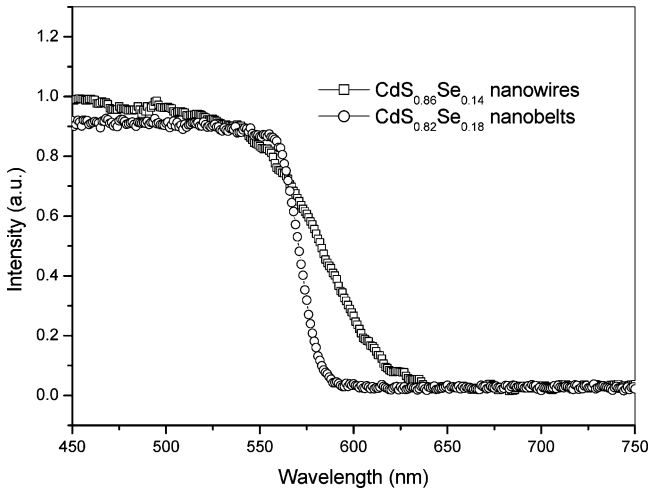

Figure 6. UV−vis absorption spectra of the $CdS_{0.86}Se_{0.14}$ nanowires and the $CdS_{0.82}Se_{0.18}$ nanobelts, respectively.

The broken lines in Figure 5 give the theoretical results of redshift versus transport distance for the $CdS_{0.86}Se_{0.14}$ wires, calculated with different values of the disorder parameter σ_0, 1.6 (for the corresponding bulk single crystal[23]) and 0.6, respectively. The solid rectangles are the corresponding experimental value for comparison. Apparently, the theoretical results using the bulk σ_0 value are a lot smaller than the experimental results, whereas the results using the smaller σ_0 value (0.6) are very close to the measured ones. The contrast between the theoretical and experimental results demonstrates that the degree of disorder in the poorly crystallized nanowires is especially high and can be comparable to those of CdSSe nanocrystals.[24] The very large disorder in the wires can be also reflected by their UV−vis absorption spectra (Figure 6), which show that the $CdS_{0.86}Se_{0.14}$ nanowires have a broader absorption edge (a larger Urbach tail) than that of the $CdS_{0.82}Se_{0.18}$ nanobelts. It is the large disorder that induces the wires having extraordinary large PL redshifts. Actually, the doping content of Se in the nanowires is smaller than those in the doped belts, which indicates that the composition-related structural disorder in the wires is smaller than those in the doped belts. The abnormally large disorder should come from the large amount of defects and dislocations in the wires, which can be seen clearly in the HRTEM image (see Figure 1d). Such defect-related local structural disorder in the wires comes mainly from their very low growth temperature, and may also come from the size effects, which can bring more structural defects in nanowires than in nanobelts.[24] Overall, it is this larger defect-related disorder that finally induces the more-pronounced PL redshift effect in the wires than in the belts.

Our work demonstrates that the band edge PL of 1D CdS-based semiconductor nanostructures can have a significant redshift during its transport along the axis, and the magnitude of redshift can be tuned by the composition or doping content, the crystallization degree, and the PL transport distance. It is worth to note, despite of the existing large disorder in these semiconductor nanostructures, the PL photon can still be guided to a very long distance away (several hundred micrometers) under the excitation of a low-power continuous-wave laser, and leave enough PL intensity for detection (see Figure 2). This optical phenomenon indicates that the doped 1D CdS nanostructures may have potential applications in color- or frequency-tunable nanodevices and broad spectral responsing devices, such as multicolor light-emitting diodes or nanolasers, photoelectric devices, and frequency transformation devices. The color/frequency of the output light/signals can be tuned by the composition (doping), the crystallization degree, the length of the nanostructures, or changing the effective transport distance.

In summary, the optical-transport properties of 1D Se-doped CdS nanostructures with different doping contents or crystallization degrees were investigated in detail using scanning near-field optical microscopy (SNOM). The results show that the locally excited PL photon can effectively propagate several hundred micrometers away, with detectable optical intensity. The guided PL shows significant redshift with the transport distance in all of these structures, and the magnitude of redshift is strongly related to the content of doping and the crystallization degree of the structures. Theoretical results using the fundamental absorption rule of semiconductors shows that the redshift magnitude is greatly dependent on the degree of structural disorder in the materials, which is in good agreement with the experimental observations. These interesting optical properties of 1D Se-doped CdS nanostructures indicate their potential applications in color-tunable nano light-emitting and/or frequency-converting devices. This work also indicates that, by doping or controlling the local microstructure, 1D semiconductor nanostructures may exhibit many more new properties and could find even wider applications in nanoscaled devices.

Acknowledgment. We are grateful for the support of NSFC of China (Term No. 90606001, 90406024 and 10574002), National 973 Project (Term No. 2002CB713802, 2007CB310500, and 2007CB936800), project of MOE of China (No.705040), the 985 fund of HNU, and the Alexander von Humboldt Foundation.

Note Added after ASAP Publication. This paper was published ASAP on August 29, 2007. A term number was added in the Acknowledgment. A discrepancy regarding nanobelts in Figure 6 was corrected. The revised paper was reposted on September 4, 2007.

Supporting Information Available: The schematic setup of optical-transport experiments, the XRD patterns, and the UV−vis absorption spectra of the as-prepared nanobelts. This material is available free of charge via the Internet at http://pubs.acs.org.

References

(1) Hu, J.; Odom, T. W.; Lieber, C. M. *Acc. Chem. Res.* **1999**, *32*, 435.
(2) Duan, X.; Huang, Y.; Cui, Y.; Lieber, C. M. *Molecular Nanoelectronics*; Reed, M. A., Lee, T., Eds.; American Scientific Publishers: New York, 2003.
(3) Yao, Z.; Dekker, C.; Avouris, P. *Top. Appl. Phys.* **2001**, *80*, 147.
(4) Dai, H. *Acc. Chem. Res.* **2002**, *35*, 1035.
(5) Huang, Y.; Duan, X.; Lieber, C. M. *Small* **2005**, *1*, 142.
(6) Law, M.; Sirbuly, D. J.; Johnson, J. C.; Goldberger, J.; Saykally, R. J.; Yang, P. *Science* **2004**, *305*, 1269.
(7) Barrelet, C. J.; Greytak, A. B.; Lieber, C. M. *Nano Lett.* **2004**, *4*, 1981.
(8) Sirbuly, D. J.; Law, M.; Pauzauskie, P.; Yan, H.; Maslov, A. V.; Knutsen, K.; Ning, C.; Saykally, R. J.; Yang, P. *PNAS*, **2005**, *102*, 7800.
(9) Huang, M. H.; Mao, S.; Feick, H.; Yan, H.; Wu, Y.; Kind, H.; Weber, E.; Russo, R.; Yang, P. *Science* **2001**, *292*, 1897.
(10) Zapien, J. A.; Jiang, Y.; Meng, X. M.; Chen, W.; Au, F. C. K.; Lifshitz, Y.; Lee, S. T. *Appl. Phys. Lett.* **2003**, *84*, 1189.
(11) Pan, A. L.; Liu, R.; Yang, Q.; Zhu, Y.; Yang, G.; Zou, B. S.; Chen, K. *J. Phys. Chem. B* **2005**, *109*, 24268.
(12) Pan, A. L.; Liu, R.; Zou, B. S. *Appl. Phys. Lett.* **2006**, *88*, 173102.
(13) Duan, X. F.; Huang, Y.; Agarwal, R.; Lieber, C. M. *Nature* **2003**, *421*, 241.
(14) Urbach, F. *Phys. Rev.* **1953**, *92*, 1324.
(15) Sa-Yakanit, V.; Glyde, N. R. *Comments Matter Phys.* **1987**, *13*, 35.
(16) Akimoto, R.; Kobayashi, M.; Suzuki, T. *J. Phys. Condens. Matter* **1996**, *8*, 105.
(17) Ullrich, B.; Schroeder, R.; Graupner, W.; Sakai, H. *Opt. Exp.* **2001**, *9*, 116.
(18) Pan, A. L.; Yang, H.; Yu, R. C.; Zou, B. S. *Nanotechnology* **2006**, *17*, 1083.
(19) Ullrich, B.; Bouchenaki, C. *Jpn. J. Appl. Phys., Part 2* **1991**, *30*, L1285.
(20) Mahr, H. *Phys. Rev.* **1962**, *125*, 1510.
(21) Fang, R. C. *Solid Spectra*; USTCP: Hefei, 2003.
(22) Samuel, L.; Brada, Y.; Beserman, R. *Phys. Rev. B* **1988**, *37*, 4671.
(23) Kunets, V. P.; Kulish, N. R.; Kunets, V. P.; Lisitsa, M. P. *Semicond. Phys., Quantum Electron. Optoelectron.* **2002**, *5*, 9.
(24) Pan, Z. W.; Dai, Z. R.; Wang, Z. L. *Science* **2001**, *291*, 1947.

NL0710295